Desalination and Water Treatment
www.deswater.com
doi: 10.1080/19443994.2013.797368

52 (2014) 1967–1979
February

Taylor & Francis
Taylor & Francis Group

Assessing groundwater quality in a coastal area using the GIS technique

Mervat El-Hoz[a,*], Abir Mohsen[a], Amal Iaaly[b]

[a]*Department of Civil Engineering, University of Balamand, Al-Koura, Lebanon*
Tel. +961 6930250x3971; Fax: +961 6930278; email: mervat.elhoz@balamand.edu.lb
[b]*GIS Center, University of Balamand, Al-Koura, Lebanon*

Received 30 November 2012; Accepted 8 April 2013

ABSTRACT

The objective of the study is to (1) provide an overview of present groundwater quality, (2) determine spatial distribution of the studied groundwater quality parameters using geographic information system (GIS) software, and (3) generate groundwater quality zone map for the city of Tripoli. Groundwater physicochemical and microbiological characteristics of the Tripoli City aquifer in Lebanon were evaluated over a one-year period. Twenty-four samples were collected from 24 private wells. It is the first study of its kind in Lebanon where the GIS was applied as an important tool for spatial analysis and data visualization. The groundwater quality information maps for the studied parameters (dissolved oxygen, temperature, pH, conductivity, total dissolved solid, salinity Cl^-, NO_2^-, NO_3^-, and *Escherichia coli*) and locations of the whole study area have been prepared using GIS spatial interpolation technique. The evaluation result indicates that the levels of the studied parameters were above the Lebanese standards desirable for human consumption and a great attention of the concerned parties is highly needed. Moreover, it is concluded that a combination of groundwater quality parameters and GIS methods is very useful as GIS provides efficient capacity to visualize the spatial data.

Keywords: Groundwater quality; Geographic Information System; Spatial analysis

1. Introduction

Groundwater is one of the most important natural resources as very large volumes are pumped each day for residential, industrial, agricultural, and commercial use. Its quality is a vital concern for people since it is essential for human health, socioeconomic development, and functioning of ecosystems [1–5]. The problems of groundwater quality are more severe in low-lying areas as the water level reaches few meters in some locations. Karstic aquifers are well known for their specific vulnerability to contamination, due to their particular characteristics such as thin soils, increased hydraulic conductivity, and salinization caused by seawater intrusion, including upconing effects [6,7]. This is a common problem in the

*Corresponding author.

Presented at the 6th International Conference on Water Resources in Mediterranean Basin (WATMED6), 10–12 October 2012, Sousse, Tunisia

1944-3994/1944-3986

Mediterranean coasts and in other coastal areas around the world. Therefore, groundwater sampling in karst should be more frequent, especially in the wake of storms, rainy periods, or snowmelts [8,9].

Many studies have been carried out to depict the correlation coefficient of different water quality parameters [10–12], but this study applied the GIS as an important tool for spatial analysis and data visualization. Geographic Information systems (GISs) are powerful computer-aided tools for varied applications ranging from sophisticated analysis and modeling of spatial data to simple inventory and management. GIS has emerged as a powerful tool for storing, analyzing, and displaying spatial data and using these data for decision-making in several areas including engineering and environmental fields [13–16]. It has been used in the map classification of groundwater quality [17–20] as for any city, a ground water quality map is important to evaluate the water safety for drinking purposes and also as a protective warning of possible environmental health problems. The main objective of this study is to provide an overview of present groundwater quality, determine spatial distribution of the studied groundwater quality parameters using GIS software, and generate groundwater quality zone map for the city of Tripoli. ArcView 10 Software (ESRI) was used to map, query, and analyze the spatial patterns of groundwater in the city.

2. Materials and methods

2.1. Study area

Tripoli is located at latitude 34˚45´ north and longitude 35˚80´ east, and altitude from 6 to 90 m above sea level with an area of 29 km^2. The city has a complex land with approximately 350,000 inhabitants. Historically, it has been almost exclusively agricultural, but during the last four decades and like other coastal stretches, urbanization and development projects are rapidly overtaking the area at the expense of agriculture. Because of unplanned construction that took place towards the end of the twentieth century in Tripoli, the city is no more an important agriculture area. The city is divided into two high hills to the northwest and low lands to the southeast with Abou Ali River lying between them. These high hills are composed mainly of two compact urbanized areas: Abou Samra and El Kobbeh (85 and 75 m above sea level, respectively). The low land (old and new Tripoli) is a flat area with elevation less than 15 m. Old Tripoli lies at the base of an escarpment on both sides of the deeply incised gorge where Abou Ali River cuts through this escarpment. The escarpment parallels the general coastline, with a coastal plain about one to two kilometers in width at its base. Elevations range from 10 to 50 m above sea level. New Tripoli has developed towards El-Mina at an elevation between 3 and 10 meters and climbs up in the southeast to an elevation of around 85 m to reach Abou Samra. Fig. 1 shows the urban structure and topography of the city [21].

Tripoli's main water resources are Hab and Abou Halka Springs which originate from outside the city in addition to a number of local public and many private non-metered and non-treated wells that provide the city with fresh water [22]. Abou Ali River, which used to be a major waterway, is polluted and does not supply the city with water anymore. The geological formations are mainly composed of fissured karstic limestone calcareous layers that are highly permeable and allow the infiltration of water into the major underground reservoir. Tripoli enjoys a typical Mediterranean climate, where winter is cool with 71 days of rain, and summer is hot and humid. Scattered rainfall events begin to occur in October and end in May. Mean annual rainfall is approximately 700 mm [23]. At present, there are no wastewater treatment plants (WWTP) within the catchment area of the Abou Ali River. There are no sewerage networks in the surrounding areas of Tripoli that has a wastewater treatment plant and the sewage is discharged directly without treatment to the sea through short outfalls (five sea outfalls) or indirectly via coastal streams in upperlands.

2.2. Groundwater sample collection and analysis

Based on the topography of the city, Tripoli was divided into four geographical regions. The samples were distributed among these regions as follows: four samples in region I (Abou Samra [AS1–AS4 inclusive]), seven samples in region II (Kobbe [K1–K7 inclusive]), eight samples in region III (Old Tripoli [OT1–OT8 inclusive]) and three samples in region IV (New Tripoli [NT1–NT3 inclusive]). Fig. 2 shows these regions with their sampling locations. As seen in this Figure, from its name, New Tripoli is still under construction with lots of green parcels. This is the last coastal area in the city that has not been fully constructed yet. In this area, the very few blocks have their own private wells that were dug a long time ago before the Lebanese law in 2005 that prevented the construction of any private well especially in urban areas. In addition, these blocks are also connected to the public water supply network and the water treatment plant feeding the city is a few kilometers away from this area. Twenty-four (24) samples were collected twice a month for a one-year period (October 2009–September

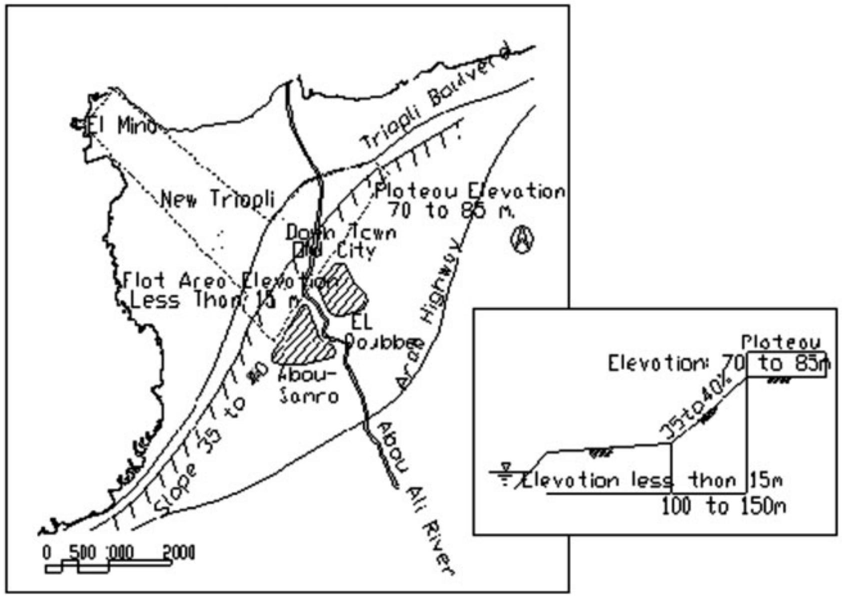

Fig. 1. Urban structure and topography of Tripoli.

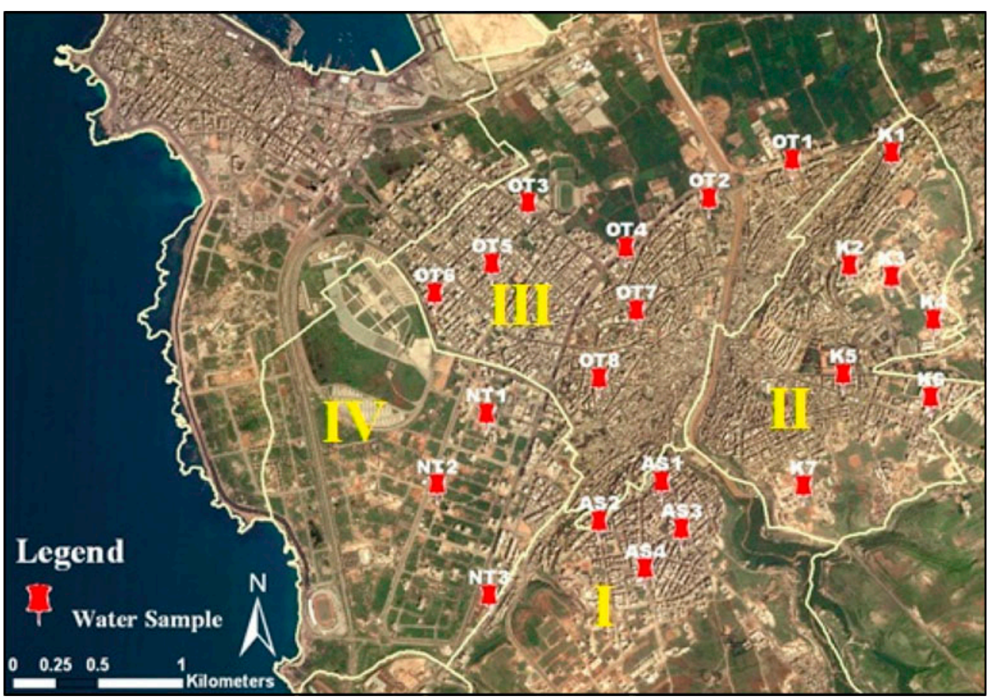

Fig. 2. The four regions of Tripoli.

2010) from 24 private wells based on 500 m radius between each well on one side and the presence of private wells in that location on the other side. These wells are not under the North Lebanon Water Establishment (NLWE) authority. A total of 23 physical, chemical, and bacteriological parameters were measured. This study will cover the analysis of only eight parameters such as dissolved oxygen (DO), conductivity, total dissolved solid (TDS), salinity, chloride, nitrate, nitrite, and *E. coli*. Microbiological constituents were collected in 500-mL sterilized glass bottles and the physical and chemical samples were collected in 500-mL polyethylene bottles. DO, conductivity, TDS, and salinity were measured on site while chloride, nitrate, nitrite, and bacteria were stored in an icebox and transported to the Environmental Engineering Laboratory at the University of Balamand for analysis. Sampling was done in accordance with the recommendations of the Standard Methods for the Examination of Water and Wastewater [24]. The field quality assurance/quality control (QA/QC) factor consisted of field blanks, equipment blanks, and duplicates while the analytical methods QA/QC factor involved the procedural blanks, laboratory duplicates, and reference samples. The concentrations of the sampled parameters were compared with the Lebanese and World Health Organization [25] standards to know the suitability of water for drinking.

2.3. Preparation of well location point feature

To develop a groundwater quality classification map, Fig. 3 presents the flowchart that was prepared for this study. The sampling locations were input in the GIS through displaying X and Y data collected from GPS. These locations were laid over the Tripoli City GIS map which used the World Geodatic System 1980 as datum and the Universal Transverse Mercator zone 36 N (North) as projection. This projected system was used to display the sampled locations in their correct locations and enhance the spatial accuracy of the data integrated in the GIS. ArcGIS software was applied in this study as an important analysis tool and visualization platform. Based on the sampling locations, a point feature showing the position of the 24 wells was prepared. The monitored water quality data (non-spatial database) were stored in excel format and linked with the spatial data by the join option in ArcMap. The spatial and the non-spatial databases formed are integrated for the generation of spatial distribution maps for the water quality parameters.

2.4. Groundwater quality mapping

To display the various pollution parameters based on different indicators in all seasons (fall, winter, spring, and summer), only 10 thematic pollutants' map layers in different seasons for salinity, conductivity, TDS, DO, nitrate, nitrite, chloride, and *E. coli* were produced for this study using the various visualization techniques available in the ArcGIS software. Table 1 presents the average levels of these parameters with their studied locations and their corresponding permissible limits. In order to convert the studied locations into polluted regions, Interpolation Techniques using the 24 sampled locations were applied through the Natural Breaks (Jenks) Quantitative Method using five classes. Spatial Analyst Extension was deployed in order to interpolate the vector point locations of the sampling sites into raster polluted region. Spatial Extent of the raster layer is exactly the extent of sampled locations bounded. Then, all studied pollutants factors were interpolated using Linear Kriging Interpolation Technique taking a cell size of $20 \times 20\,m^2$ with a special extent limited by the sampling locations to generate an estimated surface from a scattered set of points. The most common techniques of the interpolation methods used in spatial analysis that are available in GIS software are SPLINE, Inverse Distance Weighting (IDW), and the stochastic method of KRIGING. The SPLINE method estimates values using a mathematical function that minimizes the total surface curvature, resulting in a smooth surface that passes through the sampled points. IDW is based on the assumption that the nearby values contribute to the interpolated values than distant observations. It uses weight function that varies with a value of unity at the dispersion point to a value close to zero as the distance to the dispersion point increases. This interpolation works best with evenly distributed points. Similar to IDW, KRIGING uses a weighting, which assigns more influence to the nearest data points in the interpolation of values for unknown locations [26]. Moreover, KRIGING is based on the presence of a spatial structure where observations close to each other are more alike than those that are far apart (spatial autocorrelation) [27]. The interpolation created 10 raster data-sets with values ranging upon the technical field measurement in order to join and overlay all these layers and study the overall pollution factor in the studied area. In order to normalize all the raster layers into Equivalent Set of Values, a Reclassification Method using also the Raster Analyst Extension was used. The raster layer then needs to be reclassified into the same range of values that were chosen to be from 1 to 10. The reclassification method used here is the Weighted Linear Combination comparison model of multi-criteria evaluation where the pollutants maps created on the binding criteria, convert the raster layers into decision and derive the weights associated with them. The value 10 describes the most polluted location of the analysis and 1, the least polluted one.

2.5. Generating the groundwater quality map

The spatial integration for final groundwater quality zone mapping was carried out using ArcGIS

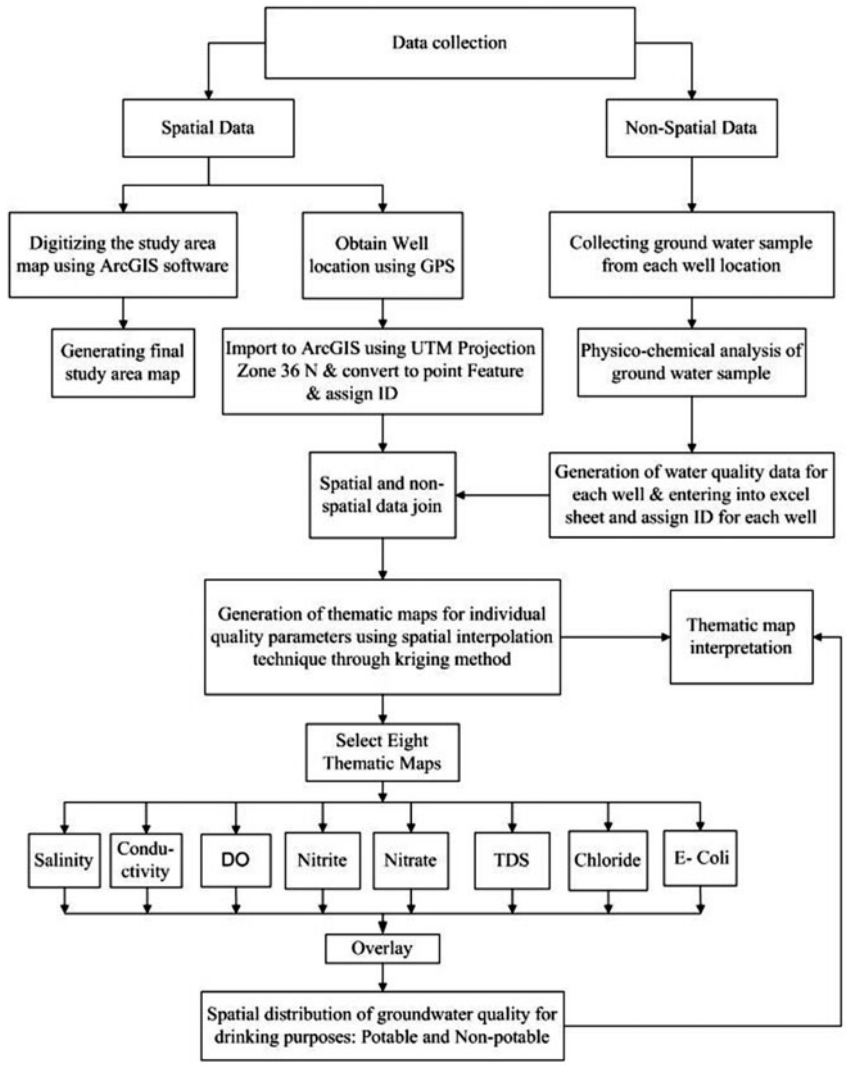

Fig. 3. Flowchart of the implemented method.

Spatial Analyst extension by overlaying the reclassified maps which are produced as a result of kriging interpolations. The GIS analysis methods were used to enhance and confirm scientifically and visually what was found in the sampling analysis.

3. Data analysis and results

Various pollution parameters based on different indicators in different seasons were displayed by adapting the symbology technique. Since data represent the value of pollution indicator at the sampled locations, quantitative symbology needs to be implemented where data are presented as dot density symbology as well as charts.

3.1. Land use pattern

There were three land use categories, i.e. grassland, cultivated land (citrus or bananas), and construction land (built-up and non-built-up) in Tripoli and the surrounding areas. The official Lebanese Government Current Land Use base map was used, and data were extracted using Arc Map. Fig. 4 shows the land use patterns in Tripoli and the surrounding areas. This map validated the hypothesis of an anthropogenic derivation for pollutants shown in Table 1. The studied pollutant concentrations in groundwater showed a systematic control of land-use characteristics which indicated the influence of anthropogenic contamination from fertilizer applications in the agricultural areas and sewage discharges in the residential areas.

Table 1
One-year average level of sampled parameters for all locations

		AS1	AS2	AS3	AS4	AS5	AS6	AS7	K1	K2	K3	K4	K5	K6	K7	Lb. Std (MCL)	WHO (MCL)
Salinity (%)	Min	0.05	0.02	0.020	0.02	0.01	0.02	0.02	0.02	0.05	0.02	0.01	0.02	0.02	0.00	0.05	0.05
	Max	0.07	0.040	0.040	0.06	0.03	0.03	0.04	0.08	0.06	0.04	0.03	0.04	0.03	0.04		
	Median	0.06	0.03	0.03	0.03	0.03	0.03	0.03	0.05	0.06	0.03	0.02	0.03	0.03	0.02		
	SD	0.01	0.00	0.007	0.011	0.01	0.00	0.01	0.02	0.01	0.005	0.01	0.01	0.005	0.01		
Cond (µS/cm)	Min	1.19	0.10	0.610	0.62	0.61	0.70	0.57	0.61	1.12	0.101	0.61	0.11	0.653	0.55	1.5	1.5
	Max	2.00	0.898	0.858	1.04	0.87	0.84	0.78	1.68	1.51	1.02	0.71	0.92	0.8	0.78		
	Median	1.47	0.85	0.71	0.73	0.80	0.81	0.63	1.33	1.36	0.8215	0.69	0.59	0.722	0.63		
	SD	0.24	0.22	0.075	0.117	0.07	0.05	0.08	0.35	0.12	0.24	0.03	0.26	0.05	0.09		
DO (mg/L)	Min	0.29	0.50	0.540	0.54	0.57	0.60	0.54	0.08	0.24	0.12	0.52	0.58	0.5	0.56	>8	>8
	Max	6.90	7.750	7.900	7.21	6.57	6.13	7.32	6.01	5.64	7.51	6.35	6.99	5.02	7.59		
	Median	0.45	0.73	0.67	0.70	0.76	0.78	0.69	0.53	0.60	0.845	0.68	0.67	0.68	0.67		
	SD	1.87	2.02	2.082	1.878	1.68	1.54	2.00	2.160	1.48	1.99	1.63	1.81	1.25	1.99		
TDS (mg/L)	Min	650	490	350	350	350	450	300	600	650	410	390.00	300.00	349	310	<500	<500
	Max	900	900	500	600	550	500	460	1,100	800	550	450.00	550.00	450	45		
	Median	755	500	405.5	400	499.5	475	400	802.5	710	495	400.00	395.00	400	31		
	SD	98.16	115.8	47.62	77.16	53.5	24	58.88	186.61	56.84	40.7	20.96	94.13	31.57	41.81		
Cl (mg/L)	Min	162.42	63.73	50.10	46.12	84.57	1.98	25.30	177.72	48.78	100.68	48.58	41.08	48.18	32.15	200	200–250
	Max	410.92	332.5	109.65	185.43	308.65	133.8354	105.89	377.29	335.07	432.90	159.62	156.23	100.91	316.73		
	Median	313.42	113.23	83.21	76.41	112.54	104.39655	77.71	224.96	242.82	155.09	63.10	120.00	66.41	56.16		
	SD	97.75	76.62	21.79	39.933	58.82	35.02	26.79	83.43	83.07	88.19	32.07	41.77	14.36	100.52		
NO_3^- (mg/L)	Min	25.86	15.60	12.51	14.87	21.50	0.60	17.11	15.01	25.06	10.99	0.00	12.19	9.12	10.26	10	10
	Max	42.60	119.13	86.11	33.39	85.98	29.2953	86.11	68.73	60.43	58.92	7.65	46.48	36.50	56.86		
	Median	33.00	33.57	19.86	22.81	24.01	25.595	24.11	42.59	41.82	18.31	5.43	17.53	18.28	19.77		
	SD	5.01	32.53	20.01	5.485	19.41	8.10	23.95	19.26	12.33	13.22	2.97	9.04	10.61	13.78		
NO_2^- (mg/L)	Min	11.38	5.67	12.912	7.25	6.51	1.26	7.70	5.60	2.28	9.92	0.00	8.88	10.19	7.37	0.1	0.2
	Max	18.00	21.54	21.543	16.77	23.00	19.34	23.11	50.01	16.98	23.76	35.20	16.19	17.61	15.90		
	Median	13.83	11.20	15.11	12.31	14.47	11.50275	13.71	13.93	10.83	14.04	15.15	14.65	13.06	13.28		
	SD	2.16	5.30	2.397	3.041	5.03	4.92	4.22	12.01	3.73	3.72	9.07	2.50	1.91	3.00		

(*Continued*)

Table 1 (*Continued*)

		NT1	NT2	NT3	OT1	OT2	OT3	OT4	OT5	OT6	OT7	OT8	Lb. Std (MCL)	WHO (MCL)
Salinity (%)	Min	0.03	0.08	0.02	0.02	0.03	0.02	0.02	0.04	0.11	0.03	0.03	0.05	0.05
	Max	0.05	0.18	0.05	0.03	0.06	0.03	0.04	0.06	0.18	0.05	0.05		
	Median	0.04	0.11	0.03	0.02	0.05	0.02	0.03	0.05	0.16	0.04	0.04		
	SD	0.01	0.03	0.01	0.00	0.01	0.00	0.01	0.00	0.03	0.01	0.01		
Cond (μS/cm)	Min	0.10	1.87	0.10	0.57	0.83	0.30	0.57	1.16	2.20	0.11	0.80	1.5	1.5
	Max	1.50	3.12	1.08	0.90	1.56	0.87	0.99	1.50	4.00	1.03	1.90		
	Median	0.91	2.27	0.89	0.63	1.24	0.62	0.86	1.26	3.23	0.97	1.12		
	SD	0.40	0.54	0.24	0.09	0.17	0.13	0.14	0.10	0.54	0.25	0.34		
DO (mg/L)	Min	0.01	0.30	0.20	0.57	0.13	0.49	0.49	0.17	0.19	0.49	0.39	>8	>8
	Max	1.10	5.73	5.18	2.29	5.70	6.34	7.19	4.76	0.69	5.68	6.89		
	Median	0.49	0.51	0.84	0.69	0.55	0.84	0.70	0.48	0.40	0.69	0.57		
	SD	0.39	1.50	1.31	0.47	1.51	1.61	1.88	1.65	0.18	1.44	1.83		
TDS (mg/L)	Min	490	1,100	410	300	500	300	350	600	1,390	500	600	<500	<500
	Max	750	2000	550	355	700	350	560	800	2,200	550	700		
	Median	545	1,550	500	311	692.5	310	499.5	700	2000	530.5	640		
	SD	77.24	340.45	37.53	19.92	59.67	17.32	69.42	54.74	320.72	23.23	32.15		
Cl	Min	60.76	123.01	64.48	35.20	77.46	34.65	36.15	77.33	528.05	55.38	100.94	200	200–250
	Max	186.21	1010.00	297.22	62.35	233.32	58.22	195.40	215.20	1080.55	103.63	167.27		
	Median	107.11	299.41	104.36	40.81	163.64	40.74	55.31	124.97	950.60	86.33	120.99		
	SD	38.67	339.79	69.36	10.81	49.89	8.31	42.58	44.70	218.98	16.85	23.05		
NO_3 (mg/L)	Min	39.12	21.34	10.45	16.37	14.27	13.24	16.91	16.19	14.56	22.11	0.00	10	10
	Max	65.02	189.15	42.23	30.95	53.66	21.02	104.50	66.30	160.86	57.69	82.22		
	Median	58.80	45.10	20.93	19.47	31.60	19.17	35.74	33.18	26.43	42.55	10.37		
	SD	8.01	66.87	8.05	4.42	12.22	3.00	27.81	15.85	52.95	11.41	30.23		
NO_2 (mg/L)	Min	8.45	5.98	8.07	9.23	9.88	0.02	8.29	8.72	5.74	9.78	0.00	0.1	0.2
	Max	17.63	17.08	23.37	18.93	22.38	20.02	76.19	22.34	23.45	19.12	255.98		
	Median	9.20	13.28	10.30	13.36	13.93	14.73	15.23	12.16	15.65	13.60	9.46		
	SD	3.76	3.87	4.67	2.93	4.22	5.21	24.04	5.13	6.70	3.24	97.09		

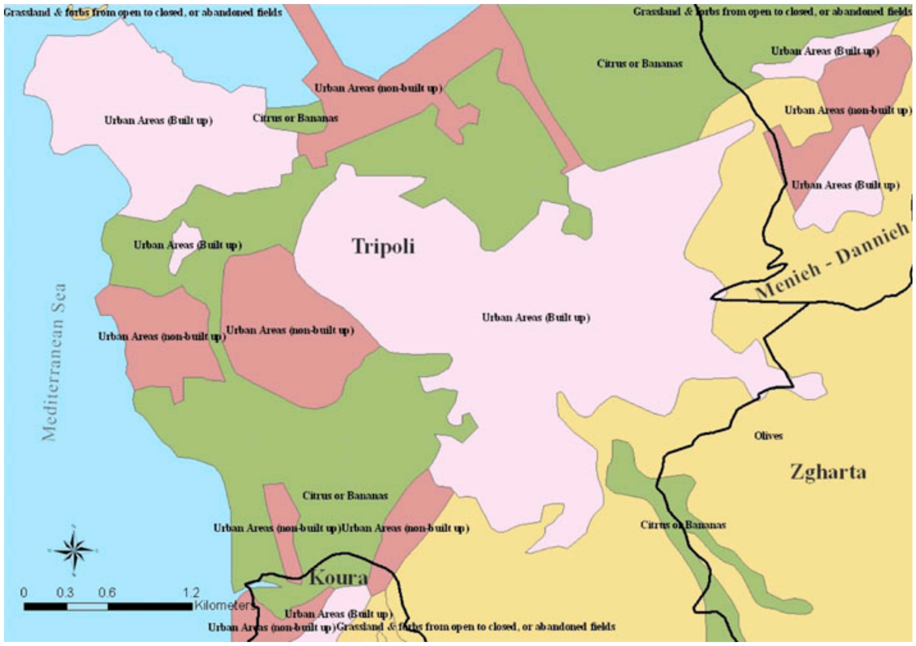

Fig. 4. Land use map of Tripoli and the surrounded regions.

3.2. TDS and DO

Figs. 5 and 6 show the TDS and DO maps with their graduate pollutant values using five classes with a Natural Breaks (Jenks) Classification Method. This classification method utilizes an algorithm to group values in classes that are separated by distinct break points. It is best used with data that is unevenly distributed but not skewed toward either end of the distribution [28]. The Natural Breaks classification method will read values of the TDS and DO from the attribute Table 1 and will display them from minimun to maximum. Five different classes were produced. As

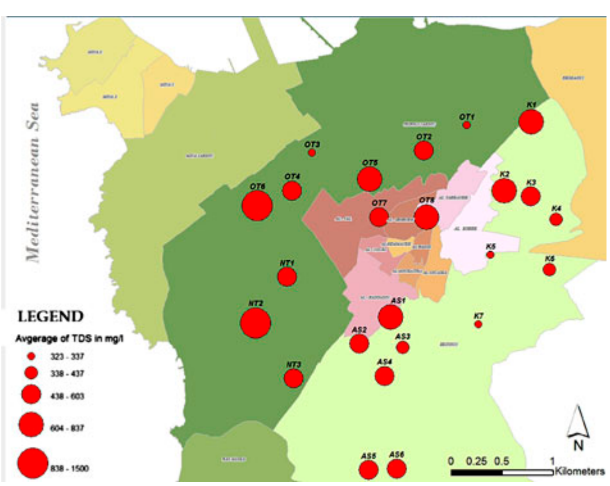

Fig. 5. Average TDS concentrations map.

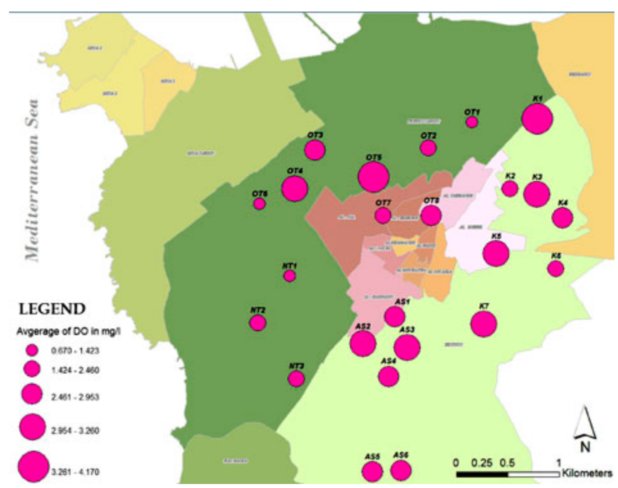

Fig. 6. Average DO map.

known, TDS is a measure of all dissolved organic and inorganic materials in water. To discover the appropriateness of groundwater for any purpose, it is important to classify the groundwater reliant upon their hydrochemical properties based on their TDS values. For TDS, the total range of the average value is between 323 and 1,500. Fig. 7 shows the Natural Breaks classification and Table 2 presents the TDS percentage for each of these classifications. According to sampling, TDS values can range from a minimum of 300 mg/L in AS7 to 2,200 mg/L; the highest values which are located in OT6 probably as a result of its

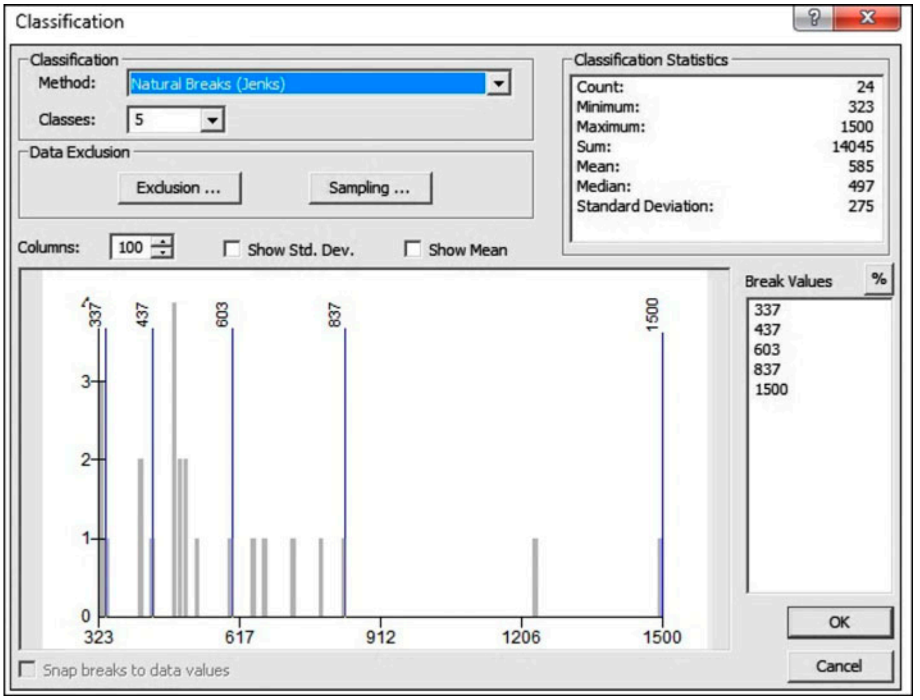

Fig. 7. TDS natural breaks classification.

closeness to the sea. Moreover, the TDS values are also found to exceed 500 mg/L, the maximum permissible limits, at many places and in all seasons which indicates the presence of soluble salts in these places of groundwater.

Concerning the DO, by applying the Natural Breaks classification, its total range of the average value is 0.670–4.170. Again Fig. 8 and Table 3 present the DO classifications and their percentages. The DO classes' map is shown in Fig. 6 where in this map, values between 0 and 2.148 represent areas with the lowest concentrations and the fifth class has values between 2.27 and 4.17 with the highest. As known, DO levels in water depend, in part, on the chemical, physical, and biochemical activities happening in water. The sampling results showed that the DO concentrations range from less than 0.1 (K1, NT1) to 7.9 mg/L (AS3) and that all of them are less than 8 ppm (the Lebanese and WHO standards) in all seasons and in all locations and the lowest levels were observed in summer season which is considered a very poor condition. This fact is due to the lack of WWTP within the catchment area. There are no sewerage networks in any of the surrounded villages except in Tripoli city where wastewater is discharged directly without treatment to the sea through short outfalls (five sea outfalls in the City of Tripoli) or indirectly via coastal streams [29]. The lack of sewerage and WWTP in these villages resulted in the discharge of raw domestic wastewater into septic tanks or directly into the Abou Ali River. Therefore, the essential source of the low level of DO are wastewater and septic system effluent, in addition to the salt water intrusion in locations near the shore, the urban runoff and the old sewer system in the city [30].

Table 2
TDS percentage for natural breaks classification

Class	Range	Percentage
1	323–337	22
2	337–437	7
3	437–603	11
4	603–837	10
5	837–1,500	50

3.3. *Salinity, nitrite, and nitrate*

In order to display the salinity, nitrite, and nitrate of the sampling locations in various seasons, a Pie Chart Symbology was used with four different readings based on various seasons. In addition, the size of the pie chart will vary based on the Sum of the Field Values; this means that the higher the concentration,

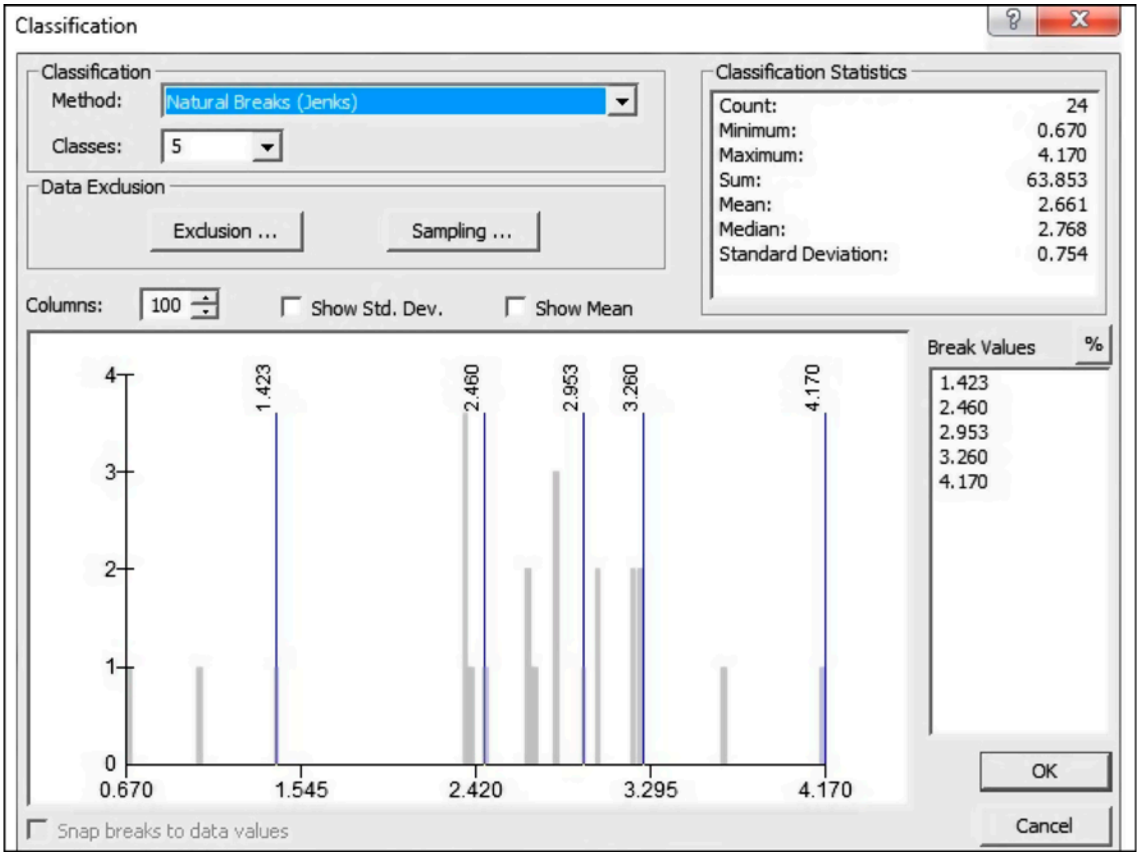

Fig. 8. DO natural breaks classification.

Table 3
DO percentage for natural breaks classification

Class	Range	Percentage
1	0.670–1.423	34.133
2	1.423–2.460	24.86
3	2.460–2.953	11.83
4	2.953–3.260	7.354
5	3.260–4.170	21.823

the bigger the size of the chart. Salinity is caused by several processes including recharge under different climatic conditions, variation in lithologic composition, ion-exchange reactions, and saltwater intrusion. Fig. 9 presents the GIS salinity map that interpret its highest values in the sampled locations close to the sea such as OT6, NT2, and K1 especially in summer season due to high pumping and subsequent lowering of the water table in the entire region and along part of the coast.

Concerning the NO_2^- and NO_3^-, the data show that their average levels in all locations and seasons exceeded those of the Lebanese and WHO standards which are 0.1 and 10 ppm. Fig. 10 displays their average concentrations in all sampled locations and the map clearly states that nitrate as the dominant

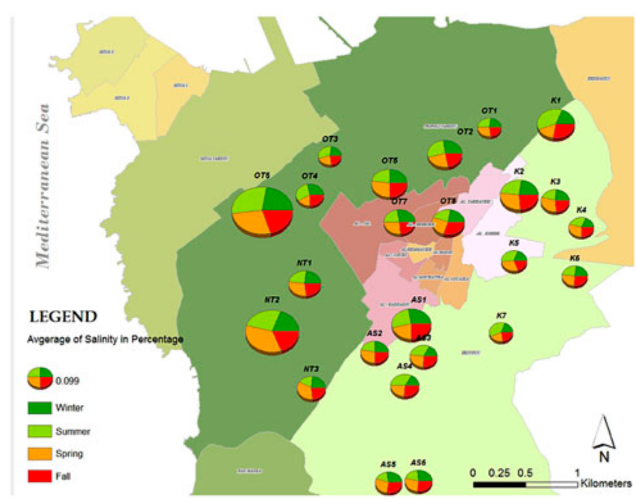

Fig. 9. Salinity map.

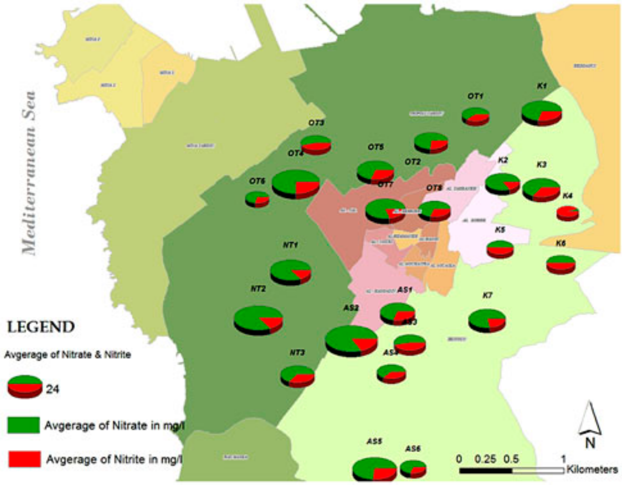

Fig. 10. Average NO_2^- and NO_3^- concentrations map.

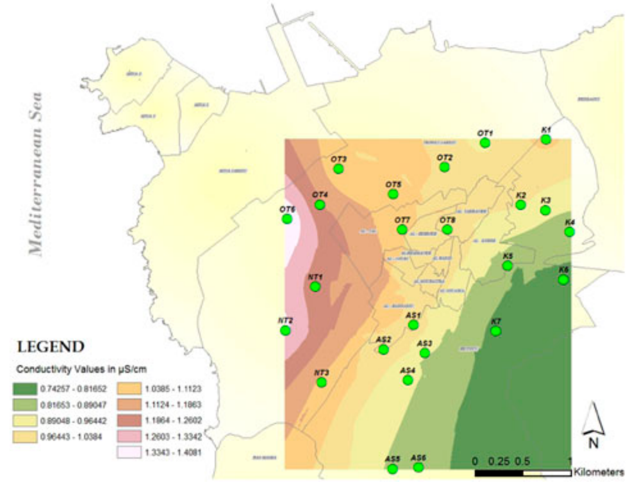

Fig. 11. Conductivity raster map.

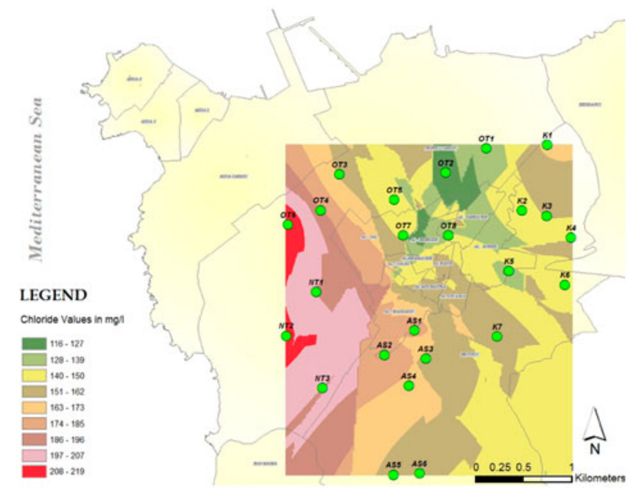

Fig. 12. Chloride raster map.

pollutant factor across the city. Nevertheless, the location K4 in Kobbeh district shows that there is an obvious non-homogenous result as the nitrate value highly exceeds the general dominant value in this studied location. This reading is an eye opener to a further analysis on two issues. The first issue is probably due to a technical misreading while the second raises a big question mark in the presence of pollutant in that area due to an unknown reason that should be further investigated. Also, locations K5 and K6 of the same Kobbeh district show an equal value of nitrite and nitrate pollutants. In downtown, the pie is bigger which means that the studied locations are polluted with local sewage from old sewer systems, natural drains carrying municipal wastes and agricultural pollution from surrounding areas in the upperland (Fig. 4).

3.4. Conductivity and chloride

In order to better understand geochemical processes that gave rise to groundwater salinity, the concentration of chloride in the sampled locations was examined. Figs. 11 and 12 show the conductivity and chloride raster maps while Fig. 13 presents the reclassification of conductivity raster map. In raster, the real measured concentration values of all produced maps are shown: with the lowest polluted locations in green and the highest polluted locations in white. Chloride concentration in natural water is commonly less than 100 mg/L unless the water is brackish or saline [31]. When examining the average chloride and conductivity in all sampled locations, it was observed that their highest concentrations exceeded the standard level (200 ppm) for chloride and conductivity (1.5 µS/cm), especially in the locations near the coast like in OT6 and NT2. Chloride occurs as a result of sea intrusion, while for conductivity, this is due to substantial contamination as a plume of contamination can move easily through the aquifer.

3.5. Final map

As mentioned above, raster calculator within Special Analyst Extension was used to add all reclassification of the raster layers in order to find zones with the highest pollution. Once all the data are normalized and reclassified into 10 different zones, the maximum and minimum pollution based on 1–10 scale of the studied region can exactly be observed

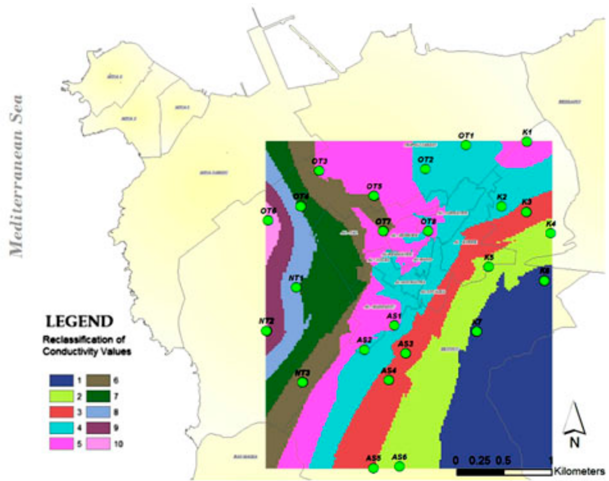

Fig. 13. Reclassification of conductivity raster map.

where 1 represents the least polluted locations and 10 the highest. After the overlay of the reclassified maps for all sampled locations with all studied parameters including the *E. coli* which exceeds the limits and renders the water unfit for human consumption, Fig. 14 is constructed from the previous raster data-sets using a Boolean addition equation and the geo-processing tools in ArcGIS raster calculator. This map is of high importance as it emphasises the fact that the underground water pollution in the Tripoli area is beyond the normal range of pollution by taking the various indicators into account. Performing Map algebra within the raster calculator for various pollutant raster layers help create a global yet alarming profile about the drastic situation of underground water in Tripoli. The values in this map are not the numbers created but the image itself

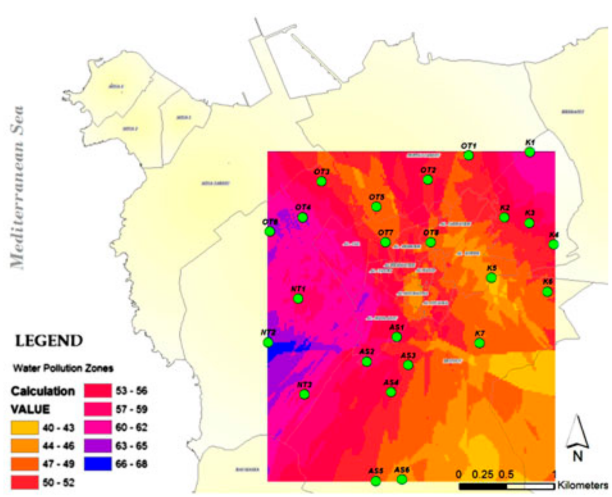

Fig. 14. Zones of groundwater pollution map.

that reflects the current situation. This map represents a catastrophic scientific analysis of groundwater quality by means of the lowest value which is much higher than the maximum allowable standard for drinking water.

4. Conclusion

Monitoring of groundwater is essential to detect and assess groundwater degradation in the highly vulnerable aquifers and to design and apply sustainable management strategies. Based on the results of the water quality parameters, the groundwater of all the sampled locations in Tripoli was found to be clearly polluted, does not comply with the standard limits for drinking water and is at high risk in terms of pollution potential. It needs great attention of all concerned parties since it is the major source of domestic, commercial, industrial and drinking water supply. The government needs to make a scientific and feasible planning for identifying an effective groundwater quality management system and for its implementation. For this, extensive public awareness and educational campaigns on the present quality crisis should be implemented without any further delay to contribute to a better and safer water usage, and the involvement and cooperation of all stakeholders in the actions of local administrators are very important.

It is important to mention that this is the first work of its kind in Lebanon and especially in Tripoli that studied the interrelation of groundwater parameters among different locations with the implementation of GIS applications. It is concluded that the combination of groundwater quality parameters and GIS methods is very useful to model the water quality-related issues as GIS provides efficient capacity to visualize the spatial data. Using ArcView's kriging and weighing methods of interpolation, maps of the contaminant concentrations were generated. Producing these maps for the sampling year allowed us to see the level of contaminated groundwater through time and in different seasons. This methodology is useful for non-environmental specialists to interpret these maps without a prior knowledge of the real measured values.

References

[1] I.S. Zektser, Groundwater and the Environment: Applications for the Global Community, Lewis, Boca Raton, 175 2000.

[2] K.N. Kim, H.J. Rajmohan, G.S. Kim, M.J. Cho Hwang, Assessment of groundwater chemistry in a coastal region (Kunsan, Korea) having complex contaminant sources: A stoichiometric approach, Environ. Geol. 46 (2004) 763–774.

[3] K. Srinivasamoorthy, C. Nanthakumar, M. Vasanthavigar, K. Vijayarag Havan, R. Rajivgan dhi, S. Chidambaram, P. Anandhan, R. Manivannan, S. Vasudevan, Groundwater quality assessment from a hard rock terrain, Salem district of Tamilnadu, India, Arabian Geosci. 4 (2011) 91–102.

[4] W.F. Humphreys, Hydrogeology and groundwater ecology: Does each inform the other? Hydrogeol. 17 (2009) 5–21.
[5] C. Steube, S. Richter, C. Griebler, First attempts towards an integrative concept for the ecological assessment of groundwater ecosystems, Hydrogeol. 17 (2009) 23–35.
[6] COST, COST Action 620, Vulnerability and risk mapping for the protection of carbonate (karst) aquifers, European Commission, Directorate-General for Research, Report EUR 20912, Luxemburg, 2003.
[7] COST, COST Action 621, Groundwater management of coastal karstic aquifers, European Commission, Directorate-General for Research, Report EUR 21366, Luxemburg, 2005.
[8] J. Vrba, Groundwater quality monitoring as a tool of groundwater resources protection, in: 21st Congress of IAH, Karst Hydrogeology and Karst Environment Protection, Geological Publication House, Beijing, China, 2, 1988, 88–97.
[9] F. Kaçaroğlu, Review of groundwater pollution and protection in karst areas, Water Air Soil Pollut. 113 (1999) 337–356.
[10] M. El-Hoz, M. Saba, Analysis of groundwater quality in kobayet region, Lebanon, Fifth International Conference on Water Resources in Mediterranean Basin (WATMED5), France, 2010.
[11] M.N. Almasri, Assessment of intrinsic vulnerability to contamination for Gaza coastal aquifer Palestine, Environ. Manage. 88 (2008) 577–593.
[12] K. Chen, J.J. Jiao, J. Huang, R. Huang, Multivariate statistical evaluation of trace elements in groundwater in a coastal area in Shenzhen, China, Environ. Pollut. 147 (2007) 771–780.
[13] D.B. Stafford, Civil Engineering Applications of Remote Sensing and Geographic Information Systems, ASCE, New York, NY, 1991.
[14] M.F. Goodchild, The state of GIS for environmental problem-solving, in: M.F. Goodchild, B.O. Parks, L.T. Steyart (Eds.), Environmental Modeling GIS, Oxford University Press, New York, pp. 8–15, 1993.
[15] P.A. Burrough, R.A. McDonnell, Principals of Geographical Information Systems, Oxford University Press, Oxford, 333 1998.
[16] C.P. Lo, A.K.W. Yeung, Concepts and Techniques of Geographic Information Systems, Prentice-Hall of India Pvt. Ltd, New Delhi, 2003, 492.
[17] M. Butler, J. Wallace, M. Lowe, Ground-water quality classification using GIS contouring methods for Cedar Valley, Iron County, Utah, in: Digital Mapping Techniques, 2002, Workshop Proceedings, US Geological Survey Open-File Report 02-370, 2002.
[18] D. Ducci, GIS techniques for mapping groundwater contamination risk, Nat. Hazards 20 (1999) 279–294.
[19] B. Nas, A. Berktay, Groundwater quality mapping in urban groundwater using GIS, Environ. Monit. Assess. 160 (2010) 215–227.
[20] S. Yammani, Groundwater quality suitable zones identification: Application of GIS, Chittoor area, Andhra Pradesh, India, Environ. Geol. 53 (2007) 201–210.
[21] Japan International Cooperation Agency (JICA), Council for development and Reconstruction (CDR), Integrated transportation plan for Greater Tripoli, 2001.
[22] M. El-Hoz, Water resources status in Tripoli, Lebanon: Problems and solutions, Fourth International Conference on Water Resources in Mediterranean Basin (WATMED4), Algeria, 2008.
[23] Central administrative of statistic, Compendium statistique national sur les statistiques de l'environnement au Liban [Central administrative of statistic, National Statistical Compendium of Environment Statistics in Lebanon], 2010.
[24] APHA-Amercican Publichealth Association, Standard Methods for the Examination of Water and Wastewater, 20th ed., Washington, USA, 1998.
[25] World Health Organization (WHO), Guidelines of Drinking Water Quality Recommendation: The Third Edition. Geneva, Vol. 2, 2006.
[26] T.P. Robinson, G. Metternicht, Testing the performance of spatial interpolation techniques for mapping soil properties, Comput. Electron. Agric. 50 (2006) 97–108.
[27] M. Azpurua, K. Dos Ramos, A comparison of spatial interpolation methods for estimation of average electromagnetic field magnitude, Prog. Electromagnet. Res. 14 (2010) 135–145.
[28] G.F. Jenks, F.C. Caspall, Error on choroplethic maps: Definition, measurement, reduction. Annals of the Association of American Geographers, vol. 61, 1971, pp. 217–244.
[29] MOE, UNDP and ECODIT, State and Trends of the Lebanese Environment, 2010.
[30] Consulting Engineers Salzgitter GMBH/Germany (CES), Bureau Technique Pour Le Development/Lebanon (BTD), Lyonnaise Des Eaux/France (LYSA), Feasibility Study for Tripoli Sewerage, Project No. 1342, Contract No. 6261, Submitted to the Council for Development and Reconstruction and Ministry of Energy and Water, 1998.
[31] C.W. Fetter, Contaminant Hydrogeology, Prentice-Hall, Englewood Cliffs, NJ, 1999.